Published in final edited form as:
Dev Biol. 2013 October 1; 382(1): 136–148. doi:10.1016/j.ydbio.2013.07.017.

Keratin 5-Cre-Driven Excision of Nonmuscle Myosin IIA in Early Embryo Trophectoderm Leads to Placenta Defects and Embryonic Lethality

James Crish[1], **Mary Anne Conti**[2], **Takao Sakai**[3], **Robert S. Adelstein**[2], and **Thomas T. Egelhoff**[1]

[1]Department of Cellular and Molecular Medicine NC10, Lerner Research Institute, The Cleveland Clinic Foundation, 9500 Euclid Avenue, Cleveland, Ohio 44195

[2]Laboratory of Molecular Cardiology, NHLBI, National Institutes of Health, Bethesda, Maryland 20892

[3]Department of Biomedical Engineering, Lerner Research Institute, The Cleveland Clinic Foundation, 9500 Euclid Avenue, Cleveland, Ohio 44195

Abstract

In studies initially focused on roles of nonmuscle myosin IIA (NMIIA) in the developing mouse epidermis, we have discovered that a previously described cytokeratin 5 (K5)-Cre gene construct is expressed in early embryo development. Mice carrying floxed alleles of the nonmuscle myosin II heavy chain gene (NMHC IIA$^{flox/flox}$) were crossed with the K5-Cre line. The progeny of newborn pups did not show a Mendelian genotype distribution, suggesting embryonic lethality. Analysis of post-implantation conceptuses from embryonic day (E)9.5 to E13.5 revealed poorly developed embryos and defective placentas, with significantly reduced labyrinth surface area and blood vessel vascularization. These results suggested the novel possibility that the bovine K5 promoter-driven Cre-recombinase was active early in trophoblast-lineage cells that give rise to the placenta. To test this possibility, K5-Cre transgenic mice were crossed with the mT/mG reporter mouse in which activation of GFP expression indicates Cre transgene expression. We observed activation of K5-Cre-driven GFP expression in the ectoplacental cone, in the extraembryonic ectoderm, and in trophoblast giant cells in the E6.5 embryo. In addition, we observed GFP expression at E11.5 to E13.5 in both the labyrinth of the placenta and the yolk sac. NMIIA expression was detected in these same cell types in normal embryos, as well as in E13.5 yolk sac and labyrinth. These findings taken together suggest that NMHC IIA may play critical roles in the early trophoblast-derived ectoplacental cone and extraembryonic ectoderm, as well as in the yolk sac and labyrinth tissues that form later. Our findings are consistent with phenotypes of constitutive NMIIA knockout mice made earlier, that displayed labyrinth and yolk sac-specific

Corresponding Author: Thomas T. Egelhoff, egelhot@ccf.org, phone 216-445-9912, Department of Cellular and Molecular Medicine, NC10, The Cleveland Clinic Foundation, 9500 Euclid Avenue, Cleveland, Ohio 44195.

defects, but our findings extend those observations by suggesting possible NMIIA roles in trophoblast lineages as well. These results furthermore demonstrate that K5-Cre gene constructs, previously reported to be activated starting at approximately E12.5 in the forming epidermis, may be widely useful as drivers for activation of cre/lox based gene excision in early embryo extraembronic trophoblast tissues as well.

Keywords

myosin; MYH9; trophoblast; placenta; keratin 5; keratinocyte

Introduction

Non-muscle myosin II (NM II) is a major motor protein that together with actin participates in a plethora of cellular and developmental processes that require force generation. The NM II holoenzyme consists of two identical heavy chains and two pairs of light chains, which in turn can assemble into higher-order bipolar filaments that assemble into the cortical cytoskeleton to produce force (Conti et al, 2004; Conti and Adelstein, 2008; Vicente-Manzanares et al, 2009). In mammals, three separate genes for the NMII heavy chains (NMHCs) associate with a common pool of light chains to produce isoforms referred to as NM IIA, NM IIB, and NM IIC (Golomb et al, 2004; Simons et al, 1991).

There have been limited studies addressing roles of NM II in the epidermis. NM II isoforms are expressed in human epidermal keratinocytes, and activated in vitro in response to wound stimuli (Betapudi et al.,2010) In Drosophila, NMII is responsible for epidermal dorsal closure during embryogenesis (Franke et al, 2005), and NM II has recently been implicated in epidermal barrier function as well (Sumigray et al, 2012). Our original goal in this work was to examine the *in vivo* role of NM IIA during epidermal homeostasis of the skin using the K5-Cre/LoxP technology, based on the established expression pattern of the K5 promoter (Blanpain and Fuchs, 2009; Byrne et al., 1994; Diamond et al., 2000; Gandarillas and Watt, 1995; Jorcano et al., 1984; Mack et al., 2005; Ramirez et al., 2004). However, our initial studies revealed that the K5Cre-directed floxed NM IIA knockout mutants were embryonic lethal and that this lethality was attributable to the fact that the K5 promoter is active in early embryogenesis with expression throughout the extra-embryonic ectoderm and in the ectoplacental cone by E6.5. This discovery led to a deeper examination of embryological phenotypes of the K5Cre-directed floxed NM IIA gene disruption.

Although NM IIA and NM IIB are essential during embryogenesis, their specific roles are not completely understood. Recent studies have shown that deletion or mutation of NMHC IIB in mice results in defects in the brain and heart with eventual death occurring between embryonic day (E)14.5 and birth (Tullio et al., 1997; Tullio et al., 2001). When NMHC IIA is deleted by germ line ablation, the embryos lack a visceral endoderm and exhibit cell-cell adhesion defects at E6.5 and eventually die by E7.5 (Conti et al., 2004; Wang et al., 2011). Interestingly, when a genetic-replacement strategy is used whereby NM IIA is replaced by NM IIB via gene-knock-in, or when chimeric forms of NM IIA (IIA head and IIB tail and vice versa) are knocked-in, placental defects occur with a failure of vascularization in the

labyrinthine layers (Wang et al., 2010; Wang et al., 2011). Similar placental defects were also observed in mutant mice that contain a knock-in mutation (R702C) in the NM IIA motor domain (Zhang et al., 2012). However, in the NM IIB knock-in mutant mouse line, the placental defects were characterized not only by a loss of fetal vascularization but a compacted, smaller labyrinth layer suggesting that this epithelial compartment which is derived from the trophoblast cell lineage could possibly be compromised as well.

The placenta is a specialized organ that facilitates the exchange of nutrients and oxygen between the mother and the fetus (Cross, 2006; Rossant and Cross, 2001; Watson and Cross, 2005). A key cell type in the placenta is trophoblast-derived epithelial cells. The trophoblast layers of the placenta arise from the outer trophectoderm of the blastocyst (Cross, 2000; Yamanaka et al., 2006). Around the time of implantation, the trophectoderm next to the inner cell mass (ICM) continues to proliferate and eventually gives rise to the extraembryonic ectoderm and ectoplacental cone (Simmons and Cross, 2005; Watson and Cross, 2005). Those trophectoderm cells away from the ICM differentiate to form the trophoblast giant cells (TGCs) (Coan et al., 2005; Simmons et al., 2007; Simmons and Cross, 2005). At around E8.5, chorioallantoic fusion occurs (Cross et al., 2003; Cross, 2006; Simmons et al., 2008). During this process, the chorion, derived from the extraembryonic membrane comes into contact with the mesoderm-derived allantois. Eventually, the trophoblasts in the chorion create folds where blood vessels grow in from the allantois. As development continues, trophoblasts and the surrounding fetal blood vessels undergo extensive villous branching to form the highly specialized compartment known as the labyrinth (Rossant and Cross, 2001). There are a number of placenta-specific genes that when disrupted affect the development of the placenta or the cell lineages that make up the placenta (Hu and Cross, 2011; Rawn and Cross, 2008; Rossant and Cross, 2001; Watson et al., 2007; Watson et al., 2011).

Our novel finding regarding the temporal and spatial expression pattern of the K5 promoter suggests that the placental defects and early embryonic lethality that we observe are due to the K5-Cre-directed ablation of the floxed NMHC IIA gene in the trophectoderm-derived cells. Therefore, our results suggest an important role for NM IIA in trophectoderm-derived cells during placenta development. Furthermore, our results suggest the possibility that the K5 promoter can be used to excise other floxed genes in trophectoderm-derived cells.

Materials and Methods

Generation of Transgenic Mouse Lines

All mice were housed and bred at the Cleveland Clinic's Biological Resource Unit following the institutional guidelines and National Institutes of Health standards. Mice were maintained on a 12-hour light/12-hour dark cycle.

To lineage trace expression of the bovine keratin 5 promoter, keratin 5-Cre ($K5^{Cre}$) mice (Honda et al., 2007; Ramirez et al., 2004) were mated with *B6.129(Cg)-Gt(ROSA)26Sor*$^{tm4(ACTB-tdTomato,-EGFP)Luo}$*/J (mT/mG* reporter mice; (Muzumdar et al., 2007)). The mT/mG reporter mouse was kindly provided by Dr. Bruce Trapp. Homozygous floxed NMHC II-A mice (II-$A^{flox/flox}$) have been described previously (Jacobelli et al.,

2010) and are available from the Mutant Mouse Regional Resource Centers (MMRRC) (#32096). Mice heterozygous for K5Cre ($K5Cre^{het}$) and homozygous for floxed NMHC IIA ($IIA^{flox/flox}$) were generated as follows: $K5Cre^{het}$ was crossed to $IIA^{flox/flox}$ to generate the bitransgenic, $K5Cre^{het}/IIA^{(flox/wt)}$. We then crossed $K5Cre^{het}/IIA^{(flox/wt)}$ with $IIA^{flox/flox}$ to generate $K5Cre^{het}/IIA^{(flox/flox)}$ knock-out mice (IIA KO).

Genotyping

Genotyping of embryos and newborn mice was determined by polymerase chain reaction (PCR). Genomic DNA was isolated from either the yolk sac of embryos or tails of newborns. The primer sequences used to identify IIA KO and wild-type alleles of NMIIA include: the forward primer 5′-GGGACACAGTTGAATCCCTT-3′ and the reverse primer, 5′- ATGGGCAGGTTCTTATAAGG-3′. The IIA excision fragment was identified using the additional reverse primer, 5′-CTCCCTTGACAGGCAGGAGAGCA-3′. Primers (forward primer: 5′-GAACATTCCACAGACCTGCA-3′, reverse primer: 5′-CCTTTGAATTGCTGGAACCC-3′) were used for detecting the K5-Cre transgene.

Antibodies

Primary antibodies used in this study include NMIIA (1:250, Covance), GAPDH (1:1000, Santa Cruz), Actin (1:5000, Sigma), Keratin 5 (1:1000, Covance), Keratin 10 (1:1000, Covance), Keratin 14 (1:1000, Covance), and alpha-6-integrin (1:1000, BD Pharmingen). The cytokeratin 8 antibody (Troma 1) was obtained from the Developmental Studies Hybridoma Bank, The University of Iowa, Department of Biology, Iowa city, IA. Secondary antibodies for immunofluorescence conjugated to Alexa 488 and Alexa-594 were purchased from Invitrogen and used at a 1:1000 dilution. Nuclei were counterstained with DAPI (Vector Lab).

Tissue preparation, Histology, and Immunofluorescence

Embryos and placentas were harvested at different gestational ages. E0.5 was defined as noon of the day in which a vaginal plug was detected. The embryonic tissues were fixed for 1 h at room temperature in 4% paraformaldehyde in phosphate buffered saline (PBS). Tissues were then rinsed three times in PBS. For paraffin embedding, tissues were dehydrated, embedded in paraffin wax and the paraffin block was cut at room temperature. For OCT embedded cryosections, tissues were cryoprotected in 30% sucrose overnight at 4°C, embedded in OCT (TFM, Electron Microscopy Sciences, Hatfield, PA) at 4°C for 1 h, and frozen in cold isopentane. The OCT blocks were stored at −80° C. Histological sections were stained with Hematoxylin and Eosin (H & E). For immunofluorescence, the tissue sections were blocked with PBS containing 1% bovine serum albumin, 0.4% TritonX-100, and 0.1% goat serum for 1 h at room temperature. The primary antibodies were diluted in PBS, added onto the slides and incubated overnight at 4°C. Following three washes in PBS, the slides were incubated with fluorescence-labeled secondary antibodies for 1 h at room temperature and washed three times. The slides were mounted using Vectashield mounting medium (Vector Lab, Burlingame Ca) and analyzed using immunofluorescence microscopy.

Confocal and Widefield Microscopy

Images were acquired with a Leica SP2 AOBS confocal microscope using an HCX PL APO 63X/1.4 N.A. oil immersion objective. Some images were also acquired with a Leica DMR widefield microscope using an HX PL APO 20X/.7 N.A> dry objective.

Western blot analysis

The isolation of the epidermis from mouse skin was prepared as described (Welter et al., 1995). Protein was extracted from the mouse epidermis using standard protein extraction methods. Briefly, the isolated epidermis was diced, placed in Laemmli lysis buffer (0.0625M Tris HCl, pH 6.8, 2% SDS, 5% β-mercaptoethanol) and sonicated briefly. Samples were centrifuged at 14,000 × g for 10 min at 4°C. The supernatants were transferred to fresh tubes and centrifuged an additional 10 min and the supernatants stored at −20°C. Epidermal extract (25 μg) was boiled for 4 min and run in 4-20% SDS-PAGE at 100 v for 1 h and then transferred to Immobilon-P (Millipore) by semidry transfer (BioRad Laboratories) at 24 v for 90 min. The membranes were incubated in blocking buffer (PBS containing 5% milk) for 2 h and probed overnight at 4°C with each primary antibody antibody. After three washes in PBS containing 0.1% Tween, the membranes were incubated with peroxidase conjugated goat anti-rabbit Ig antibodies (Thermo Scientific, Cat No. 32460) for 1 h at room temperature. After washing, the membranes were incubated with SuperSignal West Femto Maximum Sensitivity Substrate (Thermo Scientific) according to the manufacturer's instructions.

For placental and yolk sac western blots, tissue from wild type C57BL/6 embryos at E12.5 and E14.5 was extracted in RIPA buffer (Santa Cruz Biotechnology, CA) with additions to give a final concentration of 250mM NaCl, 5mM EGTA, 1mM DTT, 5mM ATP, 5mM $MgCl_2$, 10ug/ml leupeptin, 0.1mM PMSF, and 10ul/ml Sigma protease inhibitor cocktail. Tissue was homogenized with a Tissue Tearor (Biospec Products, OK), incubated on ice for 10 min and centrifuged at 14,000rpm for 10 min in a refrigerated Eppendorf centrifuge. Pellets from the centrifugation step represent material enriched for assembled cytoskeletal constituents. These pellets were resuspended in Laemmli sample buffer with 100mM DTT boiled 5 min, centrifuged for 5 min at 14,000rpm in an Eppendorf centrifuge. Supernatants were separated by PAGE in 4-12% Tris-glycine gels (Invitrogen, CA). Proteins were transferred to nitrocellulose, blocked with LiCor Blocking Buffer (Li-Cor, NE) to which anti-keratin 5 antibody (1:10,000, Covance, CA) or anti-GAPDH (1:5000, Cell Signaling, MA) was subsequently added for overnight incubation at 4 degrees. Blots were washed, incubated with fluorescence conjugated anti-mouse or anti-rabbit secondary antibody (Li-Cor), washed and fluorescence signal detected with the Li-Cor Odyssey.

Results

K5-Cre mediated excision of a floxed NMHC IIA allele results in a neonatal hyperproliferative epidermis and early postnatal lethality

In experiments designed to address the role of NM IIA in the developing mouse epidermis, we crossed previously described mice carrying floxed alleles of the NMIIA gene ($IIA^{flox/flox}$) (Jacobelli *et al.*, 2010) to mice carrying Cre-recombinase driven by a bovine

keratin 5 promoter (K5-Cre) to ablate NMHC IIA in basal epithelia. The original publication of this K5-Cre transgene construct demonstrated activation in the epidermis of E15.5 embryos, as expected for a keratin 5 promoter (Ramirez *et al.*, 2004). This transgene has been widely used to study targeted gene ablation in the epidermis and in other epithelial tissues such as the basal layer of the mammary gland duct (Eberl et al., 2012; Ferguson et al., 2012; Jackson et al., 2011; Omori et al., 2012). We crossed female $IIA^{flox/flox}$ mice with male K5-Cre/$IIA^{flox/+}$ mice to obtain homozygous floxed mice (K5-Cre/$IIA^{flox/flox}$) which are subsequently referred to in this study as IIA KO mice. As the K5-Cre transgene is expressed during oogenesis (Ramirez et al., 2004; Ramirez et al., 2004), all experiments reported in this study are based on introducing the K5-Cre transgene into embryos via male mice to avoid universal target gene excision in the fertilized zygote.

Genotype analysis of newborns revealed that offspring from mating of K5-Cre/$IIA^{flox/+}$ and $IIA^{flox/flox}$ mice did not display Mendelian genotype ratios (Table 1). Instead of the anticipated 25% Mendelian K5-Cre/$IIA^{flox/flox}$ genotype (IIA KO), we observed approximately 1% IIA KO births, represented by 2 live births from two different litters, out of a total of twenty two litters evaluated. The IIA KO newborns displayed a dramatic skin phenotype and were sacrificed by postnatal day (P) 13 for humane reasons due to increasing loss of any physical activity and lack of feeding or drinking. The skin of these IIA KO newborns over the first week was increasingly thick and rigid, and exhibited excessive scaling in addition to the lack of a hair coat as compared to the control littermate (Fig. 1A). Heterozygous pups (K5-Cre/$IIA^{flox/+}$) did not display any noticeable phenotype and are referred to as controls in this study. Histological analysis revealed that the epidermis of IIA KO newborns was thicker than that of control siblings (Fig. 1B). Fluorescence immunohistochemistry (Fig. 1C) revealed a loss of NMIIA expression in the epidermis and outer hair follicle region of the IIA KO pups (yellow arrows) as compared to the epidermis of control littermates (white arrows). Hair follicles in the IIA KO epidermis were irregular in appearance and did not display uniform orientation (Fig. 1B & C). In addition, staining intensity of alpha-6-integrin (Fig 1C, green) was consistently elevated in the epidermal and hair follicle basement membrane of the IIA KO compared to the control. Western blot analysis of protein extracts from isolated epidermis confirmed the strong reduction in NMIIA in the epidermis of IIA KO transgenic newborns (Fig. 1D).

The thickened epidermis of IIA KO pups suggested that loss of NMIIA in the epidermis may interfere with differentiation. To examine this possibility, immunofluorescence analysis was performed on P13 back skin to examine expression of a series of epidermal differentiation markers. The keratin proliferative marker, K6, not normally expressed in the epidermis, was expressed throughout the IIA KO epidermis (Fig 2 A & B). In addition, K10, which is normally expressed in the suprabasal region of the epidermis appeared to be expressed in the upper layer of the epidermis in the IIA KO (Fig 2 C & D). In contrast, the expression pattern for K14 was dramatically altered. The K14 signal is detected in the basal layer of the control epidermis, but in the IIA KO epidermis, K14 was detected in the basal and suprabasal region (Fig 2 E & F). Western blot analysis of epidermal protein extracts from control and IIA KO mice showed that the hyperproliferative keratin markers (K6 and K14) are elevated whereas the suprabasal marker (K10) is decreased in the IIA KO (Fig 2G). Suprabasal Ki67 staining

was observed in epidermis of IIA KO pups, further demonstrating a hyperproliferative defect in these mice (Fig. 3). These observations taken together suggest that ablation of NMIIA in the epidermis results in the loss of epidermal homeostasis resulting in a hyperproliferative epidermal phenotype.

The mammalian epidermis is renewed from epidermal stem cells. These stem cells express high levels of active integrin ß1 and are normally confined to the basal layer of epidermis (Alonso and Fuchs, 2003; Watt et al., 2006). To determine whether an abnormal differentiation of keratinocytes is linked to the abnormal distribution of epidermal stem cells, we next examined the localization of activated integrin ß1 positive cells via immunostaining with antibody 9EG7, which recognizes only activated integrin ß1 (Lenter et al., 1993; Honda et al., 2007). This analysis showed that integrin ß1-positive cells in the mutant epidermis were present not only in the basal but also the suprabasal layer with an increase in number (Fig. 4), suggesting that the loss of NMIIA might affect differentiation at the level of stem cells in the interfollicular epidermis.

Defective embryo development and placentas in IIA KO mice

The non-Mendelian genotype ratios that we observed for the newborn mice suggested lethality in the IIA KO embryos. To further investigate the time when the IIA KO embryos died, we examined embryos and placentas from crosses between K5-Cre/IIA$^{flox/+}$ males and IIA$^{flox/flox}$ female mice at E9.5, E10.5 and E11.5. In contrast to the normal embryos, the IIA KO embryos were markedly reduced in size and were malformed. In some cases the embryos appeared to have been resorbed (Table 2). Interestingly, many embryos appeared dead as early as E9.5 (i.e., no detectable heart beat) suggesting that K5-driven Cre-recombinase activity occurred very early in embryonic development (Fig 5A). In addition, gross morphological examination of the placentas revealed that the IIA KO placentas were smaller and less developed. Moreover, the IIA KO placentas exhibited a severe loss of vascularization (Fig 5B). These results suggest that in most embryos, lethality is occurring early during development perhaps due in part to defects in placental development.

Labyrinth and blood vessel development in the IIA KO placenta are severely reduced

To determine the morphological defects of the IIA KO placenta, we collected sagittal histological sections of the placenta from crosses between K5-Cre/IIA$^{flox/+}$ males and IIA$^{flox/flox}$ females at E12.5. A representative DAPI gray-scaled image of control placenta reveals a well-developed labyrinth characterized by a large surface area (Fig 6A). In addition, the control trophoblast giant cells (TGCs) surround the labyrinth in an ordered arrangement. In contrast, the IIA KO placenta has a poorly developed labyrinth (white line) and a discontinuous and disorganized layer of TGCs (Fig 6B). To better address the morphology of the labyrinth, sagittal placenta sections were stained with hematoxylin-eosin (H & E). The trophoblasts in the control labyrinth (green arrowheads in Fig 6C & E) are arranged in an organized manner associated with fetal blood sinuses. In addition, an extensive sinus network is observed in the control labyrinth (Fig 6C, E, yellow arrowheads). By contrast, the IIA KO labyrinth (Fig 6D, F) exhibits tightly packed trophoblast cells (yellow arrows in Fig 6F) and a poorly developed labyrinth vascular network. These data imply that the defects observed in the IIA KO embryos may be related to defective labyrinth

vascularization. This phenotype is reminiscent of earlier analysis of embryos in which nonmuscle myosin IIB (NMIIB) was swapped into the NMIIA locus to force expression of the IIB isoform in place of NMIIA in early development (Wang *et al*, 2010). That work demonstrated critical roles for NMIIA in placental vascularization that could not be rescued by the NMIIB isoform. The observation of placental defects at this early stage of placental development in the current study was unexpected, given that the K5-Cre transgene used is widely believed to be epithelial specific and to first activate in the epidermis at a later stage of embryogenesis.

Crosses with a double fluorescence reporter mouse demonstrate K5-Cre expression in trophoblast-derived lineages as early as E6.5

The trophoblast cell disorganization in the IIA KO labyrinth raised the interesting possibility that the K5 promoter driving Cre recombinase expression is active in trophoblast-lineage derived cells of the placenta. The original publication of this transgene construct reported expression in the periderm of E12.5 embryos and the basal cell layer of the adult epidermis (Ramirez *et al.*, 2004) but earlier stages were not examined. To address possible earlier expression in embryos, we utilized a double-fluorescence Cre reporter mouse, which has a Cre-responsive membrane-delimited Tomato Red fluorescence protein (mT)/membrane-delimited Green fluorescence protein (mG) construct integrated at the ROSA26 locus (mT/mG reporter mouse). In this mouse, any cells that express Cre recombinase convert their fluorescence color from red to green (Muzumdar *et al.*, 2007). We first examined K5-Cre transgene activation in the embryonic epidermis at E10.5, E11.5 and E13.5. Consistent with the original description of this K5-Cre transgene, we observed GFP expression in the basal layer of the developing epidermis by E11.5, and very intense and uniform GFP expression in the basal cells of the epidermis by E13.5 (Fig. 7). This result is consistent with the temporal and tissue-specific expression pattern not only of the original K5-Cre construct but also with established expression patterns for the endogenous K5 gene (Byrne *et al.*, 1994). No GFP expression was detected in the developing dermis of these embryos.

In view of the defects in labyrinth expansion, trophoblast giant cell distribution, and vascularization in the IIA KO embryos, we used the mT/mG mouse to examine K5-Cre expression in trophoblast lineage-derived cells of the placenta starting at E6.5. K5-Cre:mT/mG embryos were collected at E6.5 and sagittally sectioned (Fig 8A). At this stage, strong GFP expression was seen in cells of the trophectoderm surrounding the embryo and in cells located in the ectoplacental cone and extraembryonic ectoderm (Fig 8B). GFP expression was never detectable in mT/mG embryos at this stage (or any other stage) in the absence of the K5-Cre transgene. These results demonstrate that K5-Cre transgene expression occurs in trophoblast lineage-derived cells, beginning as early as E6.5.

We next asked whether endogenous K5 expression occurs in the E6.5 embryo. Laser scanning confocal immunofluorescence analysis of E6.5 embryos with an anti-K5 antibody revealed significant immunoreactivity (red) localized to the ectoplacental cone and trophectoderm region (Fig 9A) above the background signal observed when primary antibody was omitted (Fig 9B). These results demonstrate the novel finding that endogenous K5 is expressed in trophoblast-derived cells of the developing embryo as early as E6.5.

K5-Cre is expressed in multiple trophoblastic cell types of the placenta and yolk sac

To assess K5-Cre activation at later stages of development, sagittal sections of E10.5, E11.5 and E13.5 placentas were prepared and examined for activation of the mT/mG reporter expression. The H & E-stained placentas shown in Fig 10A & 10B serve as a guide, indicating placental locations examined from other sections for fluorescence. The black boxes in Fig 10A & B indicate the locations of the three major cell types examined: spongiotrophoblasts (SPs); trophoblast giant cells (TGCs); yolk sac (YS). GFP expression indicating K5-Cre transgene activation was observed as early as E10.5 in the spongiotrophoblasts (SP) of the labyrinth (top panels). By E13.5, the GFP signal was very strong in these cells (Fig 9A). In the yolk sac, scattered cells expressed GFP by E11.5, and strong GFP expression was detected in widespread patches of the yolk sac by E13.5 in K5-Cre:mT/mG embryos (Fig 10A). GFP expression was also detected in the TGCs surrounding the labyrinth at all three times examined (Fig 10B). In control analyses, GFP expression was never observed in these tissues or anywhere else in mT/mG reporter mouse embryos in the absence of the K5-Cre transgene (not shown). In sum, the activation of the mT/mG switch to GFP expression in multiple trophoblast-derived lineages in response to the K5-Cre transgene suggested that the K5 promoter specific-deletion of NMHC IIA may be occurring in early trophoblast lineage-specific development in the IIA KO embryos.

The activation of the bovine K5-Cre transgene used in our studies was not predicted, given the expectation based on many publications, that endogenous K5 expression should first be observed in embryos in the epidermis, starting around E9.5 to E10.5 (Byrne et al., 1994; Lu et al., 2005; Ramirez et al., 2004). We therefore performed immunohistological analysis to reexamine whether endogenous keratin 5 expression could be detected in early mouse embryos. Although weak, a clear positive signal above background was detectable in these tissue layers when control embryos were probed with an anti-keratin 5 antibody, with a detectable signal in trophoblast cells of the labyrinth and in the yolk sac (white arrows) (Fig 11A). As a negative control, no immunoreactivity was observed when a primary antibody directed against K10 was examined under identical staining and imaging conditions (Fig 11B). While expression of endogenous K5 was clearly present, this signal was weak as compared to epidermal expression in the same embryos by E12.5 (Fig 11C), possibly explaining why earlier studies did not recognize this placental expression pattern. Western blot analysis with kertain 5-directed antibodies further confirmed expression of this protein in placenta and yolk sac (Fig 11D). In sum, this analysis demonstrates that trophoblasts of the labyrinth and yolk sac express K5 but at a significantly lower level relative to K5 expression in the E12.5 epidermis. To our knowledge, this is the first report indicating that K5 is present in trophoblast cells of the labyrinth and yolk sac. Together, our results demonstrate expression of the K5-Cre transgene not only in the E6.5 trophoblast lineages, but also in the trophoblast-derived cells of the placenta and yolk sac at later stages. This work furthermore demonstrates that this expression parallels expression of endogenous K5 in these same cell types.

NMIIA expression is significantly decreased in the IIA KO yolk sac at E12.5

Given the robust GFP signal detected in the E13.5 yolk sac of the K5-Cre:mT/mG embryos, we examined yolk sacs from the K5-Cre/ NMHC IIA$^{flox/flox}$ embryos for NMIIA

expression. In control yolk sacs, NMIIA is expressed in the cytoplasm and along the cortical regions of cells (Fig. 12A & B). In contrast, in the IIA KO yolk sac NMIIA signal was significantly reduced (Fig. 12C & D). The endothelial cells in both the control and IIA KO yolk sacs show a strong immunoreactive signal to the NMIIA antibody. Although these results indicate that K5-directed deletion of NMHC IIA occurs in the IIA KO yolk sac by E13.5, significant defects in development are detected as early as E9.5 (Fig. 5). Although limited tissue amounts precluded genotyping to directly assess developmental consequences of NMIIA deletion at E6.5, the observation of mT/mG conversion by E6.5 suggests that loss of NMIIA in trophoblastic tissue from days E6.5 to E9.5 may be the primary driving problem leading to lethality in IIA KO embryos.

Discussion

In studies initially focused on the role of NM IIA in the mouse epidermis, we have discovered that a widely used keratin 5-Cre transgene is unexpectedly activated during early embryogenesis in trophectoderm-derived epithelial cells and in epithelial cells derived from the extraembryonic endoderm. Mouse conceptuses at the early blastocyst stage (E4.5) develop into three distinct lineages: first, the trophectoderm (polar and mural), second, the inner cell mass (ICM) that will eventually give rise to the developing embryo, and third, the primitive endoderm responsible for the development of the parietal and visceral endoderm. ICM lineages thus give rise to essentially all embryonic cell types, and contribute to extraembryonic tissues such as the placenta and yolk sac. The trophectoderm contributes to most of the extraembryonic cells, including giant cells, the ectoplacental cone, and the extra-embryonic ectoderm (Cross, 2000; Cross et al., 2003; Cross, 2006; Senner and Hemberger, 2010; Yamanaka et al., 2006). It is this trophectoderm derived component in combination with the allantoic mesoderm of the embryo that eventually gives rise to the labyrinthine layer, a complex structure of intertwined blood vessels and sinuses that mediates nutrient transfer from the maternal side to the embryo. The original report of global NM IIA disruption in mouse embryos revealed a clear and intriguing defect in the formation of the ICM-derived visceral endoderm (VE) by E6.5. In NM IIA$^{-/-}$ embryos, this epithelial layer, normally well-organized with basal/apical polarity, was poorly organized (Conti *et al.*, 2004). Subsequent differentiation of the VE was defective, indicated by lack of expression of a series of markers such as apo-AI, apo-B, α-fetoprotein, and retinal-binding protein.

In subsequent studies by Wang and colleagues, a NM IIB cDNA was knocked-in to the NMHC IIA locus, to ask whether essential roles of NM IIA at E6.5 could be complemented by the NM IIB isoform. Knock-in embryos in fact were rescued at this stage, evidenced by restoration of polarized VE at E6.5 with uniform E-cadherin junctions (Wang *et al.*, 2010). However, these embryos failed at E9.5 to E12.5, with defects in placental development that included failed angiogenesis throughout the embryo and failed development and expansion of the labyrinthine layer. This analysis demonstrated an isoform-specific requirement for NM IIA in placental function and global angiogenesis throughout the embryo. Our unexpected targeting of NM IIA disruption in early embryo trophoblast lineages has led to a phenotype reminiscent of that of Wang and colleagues. Notably, we did not observe defects in organization of the visceral endoderm, but we did observe that the IIA KO placentas have an underdeveloped labyrinth in addition to a lack of fetal blood spaces and maternal blood

sinuses. Our results substantiate the earlier results and importantly, further argue that NM IIA has critical roles in the trophoblast lineages during these processes as our K5-Cre conditional knockout appears not to affect ICM-derived lineages through this period of development.

The bovine keratin 5-Cre transgene used in our work has been used in a number of earlier conditional gene disruption studies targeting the epidermis (Chrostek et al., 2006; Essayem et al., 2006; Grose et al., 2007; Jackson et al., 2011; Omori et al., 2006; Omori et al., 2012). Most of these publications were either silent regarding any observations of embryonic lethality, or in a few cases commented that pups were born at normal Mendelian ratios. One report, focused on mammary gland disruption of the tumor suppressor Wwox did report unexplained premature lethality in males and females that was independent of mammary gland development (Ferguson *et al.*, 2012), possibly consistent with unrecognized K5-Cre expression at an earlier stage of development. We speculate that the lack of early embryonic defects in most published studies further reflects the critical and non-redundant roles of NM IIA in extraembryonic development, relative to other target genes that have been excised with this Cre transgene.

The limited number of live births we obtained from K5-Cre × $IIA^{flox/flox}$ crosses (two) limits our ability to draw conclusions regarding the role of NM IIA in epidermal development. However, it is intriguing that both pups displayed hyperproliferative skin and defective hair follicle formation. These phenotypes are reminiscent of earlier studies where cell-cell junction constituents have been subjected to epidermal-restricted knockout. For example, epidermal disruption of the adherens junction protein α-catenin leads to epidermal disorganization, hyperproliferation, epidermal thickening, as well as defects in stratification (Vasioukhin et al., 2001a; Vasioukhin et al., 2001b) Disruption of p120-catenin, another key adherens junction regulatory protein, similarly leads to epidermal hyperplasia and inappropriate suprabasal expression of keratin 6 (Perez-Moreno et al., 2006). We speculate that NM IIA may be a critical mediator of cell-cell junction formation in the epidermis, and its disruption results in barrier dysfunction and inflammation for similar reasons as in the earlier studies. Future studies, relying on tamoxifen-inducible Cre constructs (Indra et al., 1999), will likely be needed to address this hypothesis in depth.

In conclusion, these results extend previously reported transgenic findings demonstrating that NM IIA has an important role in placental development (Wang et al., 2010; Zhang et al., 2012), by demonstrating essential roles for NM IIA in extraembryonic lineages. It will be of interest in future studies to determine why NM IIA is critical in trophectoderm lineages. In the original NM IIA disruption (Conti *et al.*, 2004), it was established that NM IIA had a critical role in stabilizing E-cadherin cell-cell junctions, a role that could be rescued with forced NM IIB expression (Wang *et al.*, 2010). Conceivably NM IIA plays a similar role in trophectoderm and extraembryonic endoderm of the placenta and yolk sac respectively during labyrinth and yolk sac formation.

Acknowledgments

We thank Veronique Lefebvre, Oliver Wessely, and Anna-Katerina Hadjantonakis for helpful advice during the course of this project.

Reference List

Alonso L, Fuchs E. Stem cells of the skin epithelium. Proc Natl Acad Sci U S A. 2003; 100(Suppl 1): 11830–11835. [PubMed: 12913119]

Betapudi V, Rai V, Beach JR, Egelhoff T. Novel regulation and dynamics of myosin II activation during epidermal wound responses. Exp Cell Res. 2010; 316:980–991. [PubMed: 20132815]

Blanpain C, Fuchs E. Epidermal homeostasis: a balancing act of stem cells in the skin. Nat Rev Mol Cell Biol. 2009; 10:207–217. [PubMed: 19209183]

Byrne C, Tainsky M, Fuchs E. Programming gene expression in developing epidermis. Development. 1994; 120:2369–2383. [PubMed: 7525178]

Chrostek A, Wu X, Quondamatteo F, Hu R, Sanecka A, Niemann C, Langbein L, Haase I, Brakebusch C. Rac1 is crucial for hair follicle integrity but is not essential for maintenance of the epidermis. Mol Cell Biol. 2006; 26:6957–6970. [PubMed: 16943436]

Coan PM, Ferguson-Smith AC, Burton GJ. Ultrastructural changes in the interhaemal membrane and junctional zone of the murine chorioallantoic placenta across gestation. J Anat. 2005; 207:783–796. [PubMed: 16367805]

Conti MA, Adelstein RS. Nonmuscle myosin II moves in new directions. J Cell Sci. 2008; 121:11–18. [PubMed: 18096687]

Conti MA, Even-Ram S, Liu C, Yamada KM, Adelstein RS. Defects in cell adhesion and the visceral endoderm following ablation of nonmuscle myosin heavy chain II-A in mice. J Biol Chem. 2004; 279:41263–41266. [PubMed: 15292239]

Cross JC. Genetic insights into trophoblast differentiation and placental morphogenesis. Semin Cell Dev Biol. 2000; 11:105–113. [PubMed: 10873707]

Cross JC. Placental function in development and disease. Reprod Fertil Dev. 2006; 18:71–76. [PubMed: 16478604]

Cross JC, Simmons DG, Watson ED. Chorioallantoic morphogenesis and formation of the placental villous tree. Ann N Y Acad Sci. 2003; 995:84–93. [PubMed: 12814941]

Diamond I, Owolabi T, Marco M, Lam C, Glick A. Conditional gene expression in the epidermis of transgenic mice using the tetracycline-regulated transactivators tTA and rTA linked to the keratin 5 promoter. J Invest Dermatol. 2000; 115:788–794. [PubMed: 11069615]

Eberl M, Klingler S, Mangelberger D, Loipetzberger A, Damhofer H, Zoidl K, Schnidar H, Hache H, Bauer HC, Solca F, Hauser-Kronberger C, Ermilov AN, Verhaegen ME, Bichakjian CK, Dlugosz AA, Nietfeld W, Sibilia M, Lehrach H, Wierling C, Aberger F. Hedgehog-EGFR cooperation response genes determine the oncogenic phenotype of basal cell carcinoma and tumour-initiating pancreatic cancer cells. EMBO Mol Med. 2012; 4:218–233. [PubMed: 22294553]

Essayem S, Kovacic-Milivojevic B, Baumbusch C, McDonagh S, Dolganov G, Howerton K, Larocque N, Mauro T, Ramirez A, Ramos DM, Fisher SJ, Jorcano JL, Beggs HE, Reichardt LF, Ilic D. Hair cycle and wound healing in mice with a keratinocyte-restricted deletion of FAK. Oncogene. 2006; 25:1081–1089. [PubMed: 16247468]

Ferguson BW, Gao X, Kil H, Lee J, Benavides F, Abba MC, Aldaz CM. Conditional Wwox deletion in mouse mammary gland by means of two Cre recombinase approaches. PLoS ONE. 2012; 7:e36618. [PubMed: 22574198]

Franke JD, Montague RA, Kiehart DP. Nonmuscle myosin II generates forces that transmit tension and drive contraction in multiple tissues during dorsal closure. Curr Biol. 2005; 15:2208–2221. [PubMed: 16360683]

Gandarillas A, Watt FM. The 5′ noncoding region of the mouse involucrin gene: comparison with the human gene and genes encoding other cornified envelope precursors. Mamm Genome. 1995; 6:680–682. [PubMed: 8535084]

Golomb E, Ma X, Jana SS, Preston YA, Kawamoto S, Shoham NG, Goldin E, Conti MA, Sellers JR, Adelstein RS. Identification and characterization of nonmuscle myosin II-C, a new member of the myosin II family. J Biol Chem. 2004; 279:2800–2808. [PubMed: 14594953]

Grose R, Fantl V, Werner S, Chioni AM, Jarosz M, Rudling R, Cross B, Hart IR, Dickson C. The role of fibroblast growth factor receptor 2b in skin homeostasis and cancer development. EMBO J. 2007; 26:1268–1278. [PubMed: 17304214]

Honda K, Sakaguchi T, Sakai K, Schmedt C, Ramirez A, Jorcano JL, Tarakhovsky A, Kamisoyama H, Sakai T. Epidermal hyperplasia and papillomatosis in mice with a keratinocyte-restricted deletion of csk. Carcinogenesis. 2007; 28:2074–2081. [PubMed: 17494055]

Hu D, Cross JC. Ablation of Tpbpa-positive trophoblast precursors leads to defects in maternal spiral artery remodeling in the mouse placenta. Dev Biol. 2011; 358:231–239. [PubMed: 21839735]

Indra AK, Warot X, Brocard J, Bornert JM, Xiao JH, Chambon P, Metzger D. Temporally-controlled site-specific mutagenesis in the basal layer of the epidermis: comparison of the recombinase activity of the tamoxifen-inducible Cre-ER(T) and Cre-ER(T2) recombinases. Nucleic Acids Res. 1999; 27:4324–4327. [PubMed: 10536138]

Jackson B, Peyrollier K, Pedersen E, Basse A, Karlsson R, Wang Z, Lefever T, Ochsenbein AM, Schmidt G, Aktories K, Stanley A, Quondamatteo F, Ladwein M, Rottner K, van HJ, Brakebusch C. RhoA is dispensable for skin development, but crucial for contraction and directed migration of keratinocytes. Mol Biol Cell. 2011; 22:593–605. [PubMed: 21209320]

Jacobelli J, Friedman RS, Conti MA, Lennon-Dumenil AM, Piel M, Sorensen CM, Adelstein RS, Krummel MF. Confinement-optimized three-dimensional T cell amoeboid motility is modulated via myosin IIA-regulated adhesions. Nat Immunol. 2010; 11:953–961. [PubMed: 20835229]

Jorcano JL, Magin TM, Franke WW. Cell type-specific expression of bovine keratin genes as demonstrated by the use of complementary DNA clones. J Mol Biol. 1984; 176:21–37. [PubMed: 6204061]

Lenter M, Uhlig H, Hamann A, Jeno P, Imhof B, Vestweber D. A monoclonal antibody against an activation epitope on mouse integrin chain beta 1 blocks adhesion of lymphocytes to the endothelial integrin alpha 6 beta 1. Proc Natl Acad Sci U S A. 1993; 90:9051–9055. [PubMed: 7692444]

Lu H, Hesse M, Peters B, Magin TM. Type II keratins precede type I keratins during early embryonic development. Eur J Cell Biol. 2005; 84:709–718. [PubMed: 16180309]

Mack JA, Anand S, Maytin EV. Proliferation and cornification during development of the mammalian epidermis. Birth Defects Res C Embryo Today. 2005; 75:314–329. [PubMed: 16425252]

Muzumdar MD, Tasic B, Miyamichi K, Li L, Luo L. A global double-fluorescent Cre reporter mouse. Genesis. 2007; 45:593–605. [PubMed: 17868096]

Omori E, Inagaki M, Mishina Y, Matsumoto K, Ninomiya-Tsuji J. Epithelial transforming growth factor beta-activated kinase 1 (TAK1) is activated through two independent mechanisms and regulates reactive oxygen species. Proc Natl Acad Sci U S A. 2012; 109:3365–3370. [PubMed: 22331902]

Omori E, Matsumoto K, Sanjo H, Sato S, Akira S, Smart RC, Ninomiya-Tsuji J. TAK1 is a master regulator of epidermal homeostasis involving skin inflammation and apoptosis. J Biol Chem. 2006; 281:19610–19617. [PubMed: 16675448]

Perez-Moreno M, Davis MA, Wong E, Pasolli HA, Reynolds AB, Fuchs E. p120-catenin mediates inflammatory responses in the skin. Cell. 2006; 124:631–644. [PubMed: 16469707]

Ramirez A, Page A, Gandarillas A, Zanet J, Pibre S, Vidal M, Tusell L, Genesca A, Whitaker DA, Melton DW, Jorcano JL. A keratin K5Cre transgenic line appropriate for tissue-specific or generalized Cre-mediated recombination. Genesis. 2004; 39:52–57. [PubMed: 15124227]

Rawn SM, Cross JC. The evolution, regulation, and function of placenta-specific genes. Annu Rev Cell Dev Biol. 2008; 24:159–181. [PubMed: 18616428]

Rossant J, Cross JC. Placental development: lessons from mouse mutants. Nat Rev Genet. 2001; 2:538–548. [PubMed: 11433360]

Senner CE, Hemberger M. Regulation of early trophoblast differentiation - lessons from the mouse. Placenta. 2010; 31:944–950. [PubMed: 20797785]

Simmons DG, Cross JC. Determinants of trophoblast lineage and cell subtype specification in the mouse placenta. Dev Biol. 2005; 284:12–24. [PubMed: 15963972]

Simmons DG, Fortier AL, Cross JC. Diverse subtypes and developmental origins of trophoblast giant cells in the mouse placenta. Dev Biol. 2007; 304:567–578. [PubMed: 17289015]

Simmons DG, Natale DR, Begay V, Hughes M, Leutz A, Cross JC. Early patterning of the chorion leads to the trilaminar trophoblast cell structure in the placental labyrinth. Development. 2008; 135:2083–2091. [PubMed: 18448564]

Simons M, Wang M, McBride OW, Kawamoto S, Yamakawa K, Gdula D, Adelstein RS, Weir L. Human nonmuscle myosin heavy chains are encoded by two genes located on different chromosomes. Circ Res. 1991; 69:530–539. [PubMed: 1860190]

Sumigray KD, Foote HP, Lechler T. Noncentrosomal microtubules and type II myosins potentiate epidermal cell adhesion and barrier formation. J Cell Biol. 2012; 199:513–525. [PubMed: 23091070]

Tullio AN, Accili D, Ferrans VJ, Yu ZX, Takeda K, Grinberg A, Westphal H, Preston YA, Adelstein RS. Nonmuscle myosin II-B is required for normal development of the mouse heart. Proc Natl Acad Sci U S A. 1997; 94:12407–12412. [PubMed: 9356462]

Tullio AN, Bridgman PC, Tresser NJ, Chan CC, Conti MA, Adelstein RS, Hara Y. Structural abnormalities develop in the brain after ablation of the gene encoding nonmuscle myosin II-B heavy chain. J Comp Neurol. 2001; 433:62–74. [PubMed: 11283949]

Vasioukhin V, Bauer C, Degenstein L, Wise B, Fuchs E. Hyperproliferation and defects in epithelial polarity upon conditional ablation of alpha-catenin in skin. Cell. 2001a; 104:605–617. [PubMed: 11239416]

Vasioukhin V, Bowers E, Bauer C, Degenstein L, Fuchs E. Desmoplakin is essential in epidermal sheet formation. Nat Cell Biol. 2001b; 3:1076–1085. [PubMed: 11781569]

Vicente-Manzanares M, Ma X, Adelstein RS, Horwitz AR. Non-muscle myosin II takes centre stage in cell adhesion and migration. Nat Rev Mol Cell Biol. 2009; 10:778–790. [PubMed: 19851336]

Wang A, Ma X, Conti MA, Adelstein RS. Distinct and redundant roles of the non-muscle myosin II isoforms and functional domains. Biochem Soc Trans. 2011; 39:1131–1135. [PubMed: 21936777]

Wang A, Ma X, Conti MA, Liu C, Kawamoto S, Adelstein RS. Nonmuscle myosin II isoform and domain specificity during early mouse development. Proc Natl Acad Sci U S A. 2010; 107:14645–14650. [PubMed: 20679233]

Watson ED, Cross JC. Development of structures and transport functions in the mouse placenta. Physiology (Bethesda). 2005; 20:180–193. [PubMed: 15888575]

Watson ED, Geary-Joo C, Hughes M, Cross JC. The Mrj co-chaperone mediates keratin turnover and prevents the formation of toxic inclusion bodies in trophoblast cells of the placenta. Development. 2007; 134:1809–1817. [PubMed: 17409114]

Watson ED, Hughes M, Simmons DG, Natale DR, Sutherland AE, Cross JC. Cell-cell adhesion defects in Mrj mutant trophoblast cells are associated with failure to pattern the chorion during early placental development. Dev Dyn. 2011; 240:2505–2519. [PubMed: 21972064]

Watt FM, Lo CC, Silva-Vargas V. Epidermal stem cells: an update. Curr Opin Genet Dev. 2006; 16:518–524. [PubMed: 16919447]

Welter JF, Crish JF, Agarwal C, Eckert RL. Fos-related antigen (Fra-1), junB, and junD activate human involucrin promoter transcription by binding to proximal and distal AP1 sites to mediate phorbol ester effects on promoter activity. J Biol Chem. 1995; 270:12614–12622. [PubMed: 7759510]

Yamanaka Y, Ralston A, Stephenson RO, Rossant J. Cell and molecular regulation of the mouse blastocyst. Dev Dyn. 2006; 235:2301–2314. [PubMed: 16773657]

Zhang Y, Conti MA, Malide D, Dong F, Wang A, Shmist YA, Liu C, Zerfas P, Daniels MP, Chan CC, Kozin E, Kachar B, Kelley MJ, Kopp JB, Adelstein RS. Mouse models of MYH9-related disease: mutations in nonmuscle myosin II-A. Blood. 2012; 119:238–250. [PubMed: 21908426]

Manuscript Highlights

Cre-lox approaches reveal roles for myosin IIA in early epidermal formation.

Cre-lox approaches reveal roles for myosin IIA in early embryogenesis.

Conditional myosin IIA disruption causes defects in placental vascularization

Mouse keratin 5 is expressed in early embryogenesis in extraembryonic tissues

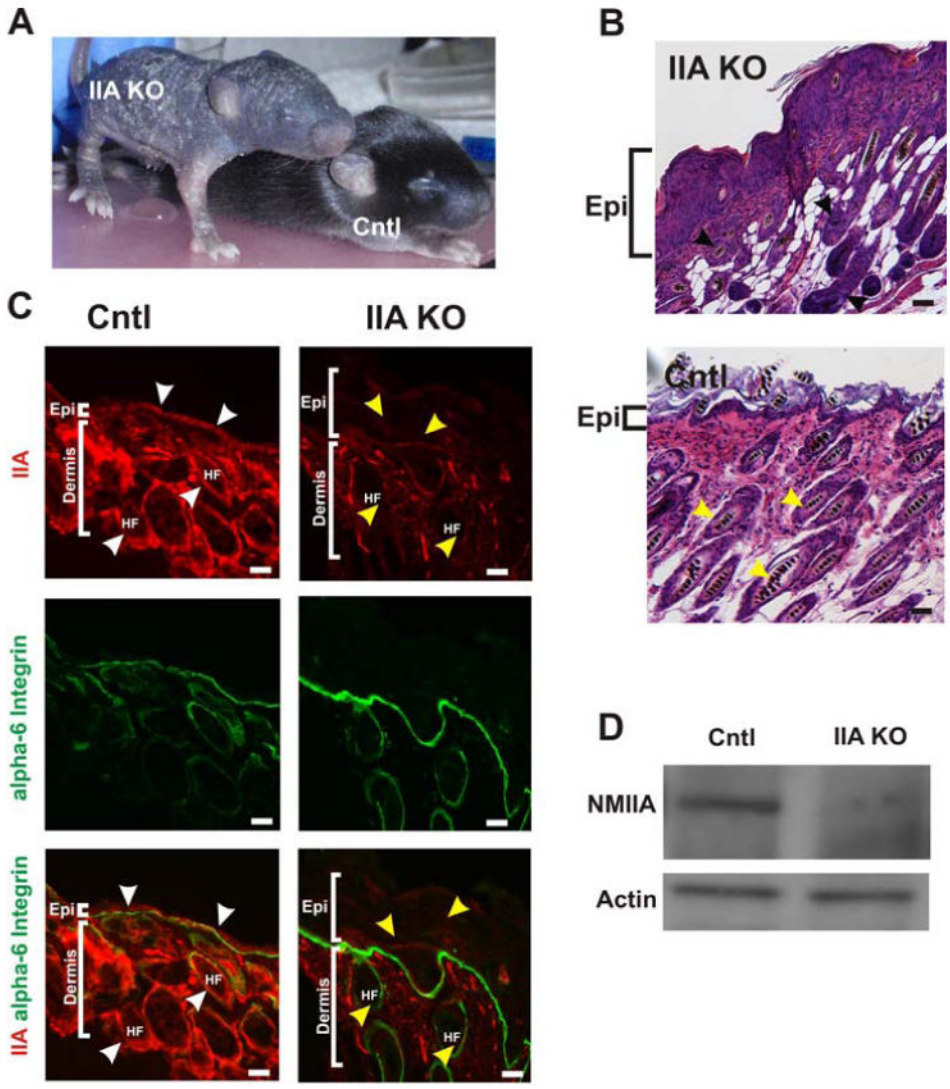

Figure 1. Conditional deletion of NMHC II-A in the epidermis leads to epidermal hyperproliferation and disruption of hair follicle development in newborn mice

(A) The IIA KO mouse at postnatal day (P)10 displayed a severely disrupted skin and hair phenotype compared to the control littermate (Cntl) (B) Hematoxylin and Eosin (H & E) stained dorsal skin from P13 reveal a thickened and hyperproliferative epidermis (Epi) in the IIA KO (top panel) compared to the littermate epidermis (bottom panel) and disorganized and disoriented hair follicle growth in the IIA KO compared to control (black and yellow arrowheads, respectively). (C) Cryosections from the dorsal skin of both control and IIA KO P13 mice were immunostained for NM IIA (red) and alpha 6-integrin (green). White arrowheads point to NMIIA localization in the epidermis and hair follicle in the control epidermis. The yellow arrowheads identify representative regions in both the epidermis and hair follicles (HF) of the IIA KO that lack NM II expression. The thickened epidermis in the IIA KO is highlighted by the white brackets. Scale bars, 25μm. (D) Immunoblot analysis of P13 epidermal extracts from control and IIA KO mice and probed with anti-NMIIA antibody and actin which serves as a loading control.

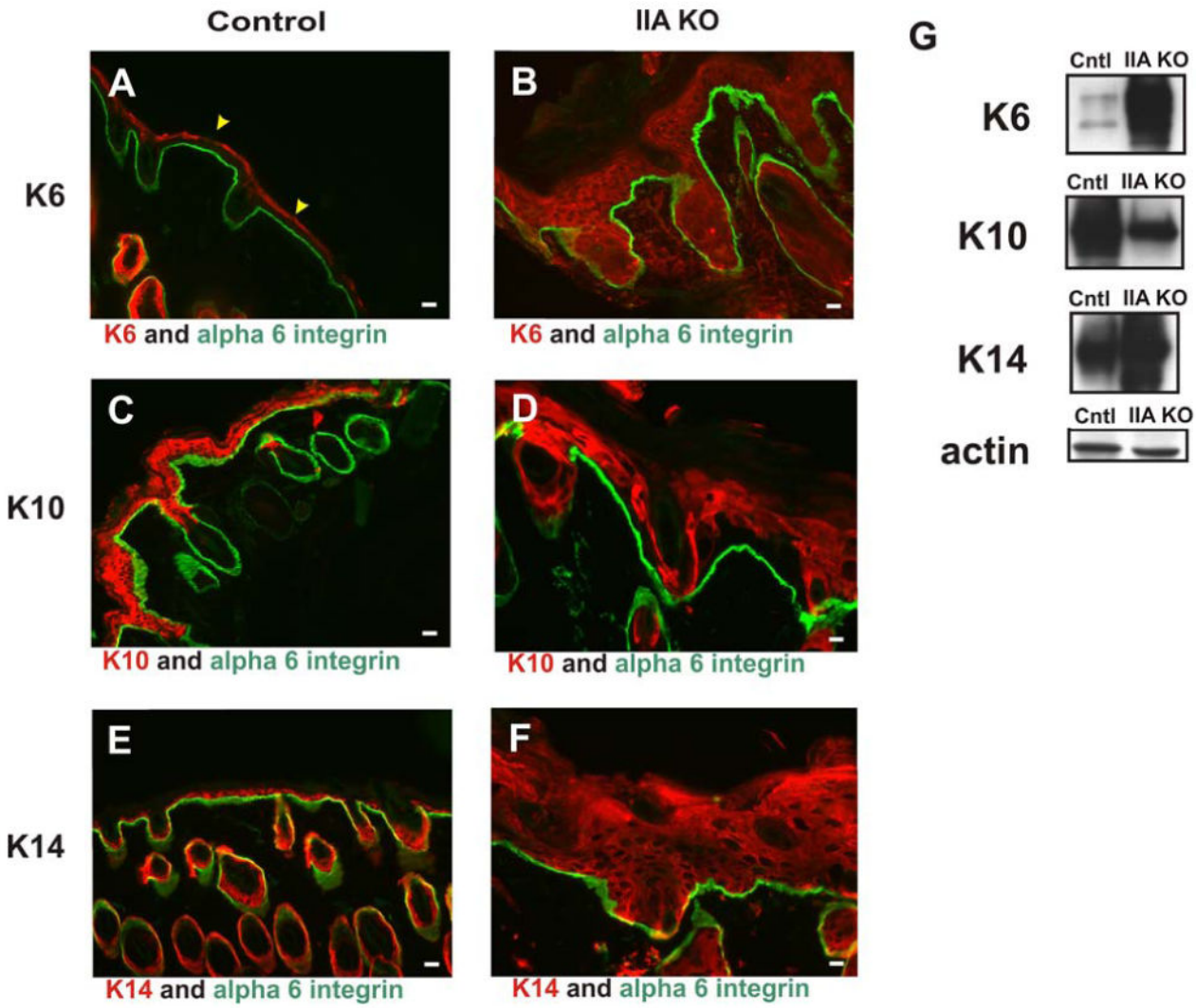

Figure 2. Epidermal homeostasis is disrupted in the P13 skin of IIA KO mice

Skin from control littermate and IIA KO P13 mice was prepared for analysis. (A, C, E) Control mouse skin stained for keratin 6 (K6, red) (A), keratin 10 (K10, red) (C), and keratin 14 (K14, red) (E). (B, D, F) IIA KO skin stained for K6 (red) (B), K10 (red) (D), and K14 (red) (F). (A to F) Control and IIA KO skin sections were also stained for alpha 6 integrin (green). (G) Western blot analyses of epidermal extracts from IIA KO mice reveal that epidermal hyperproliferation markers (K6 and K14) are elevated and K10, a marker of differentiation, is decreased compared to control lysates. Actin is shown as a loading control. Scale bars, 25 μm. Yellow arrowheads in panel (A) denote non-specific staining of the cornified envelope by the secondary antibody.

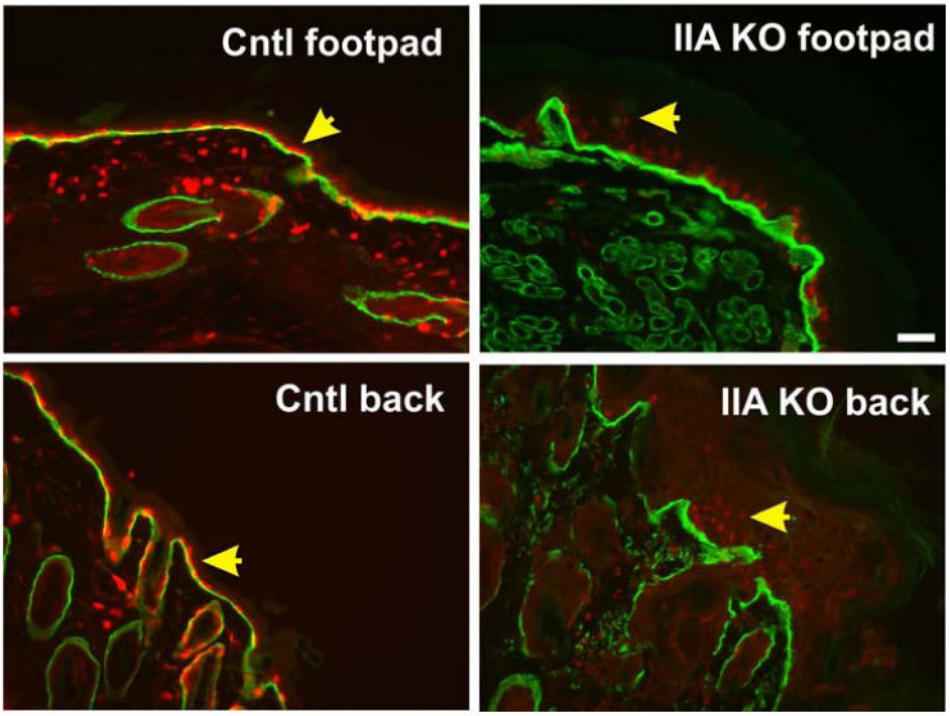

Figure 3. Surpabasal Ki67 staining in footpad and back skin of IIA KO mice

Tissues from control littermate and IIA KO P13 mice were fixed, sectioned, and stained for Ki67 (red) and alpha 6 integrin (green). Yellow arrowheads indicate single basal layer of Ki67 positive cells in control samples and suprabasal Ki67 staining in the IIA KO samples. In both locations we note that Ki67 staining, while suprabasal in the IIA KO, also displayed a weaker signal in all cells. Scale bar, 50 μm.

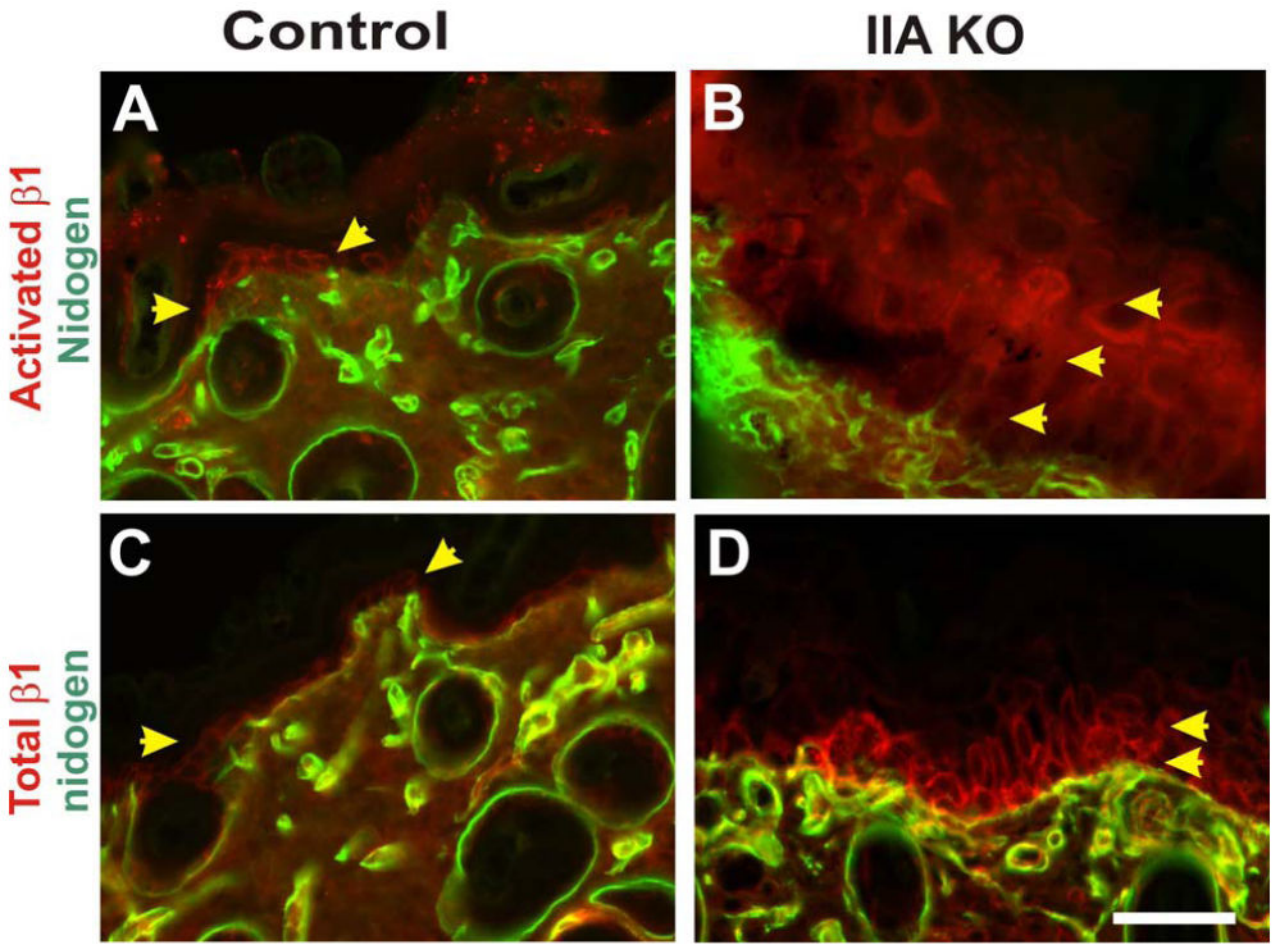

Figure 4. Epidermal loss of NMHC IIA drives suprabasal integrin ß1 activation

Skin from control littermate and IIA KO P13 mice was analyzed via immunohistochemistry on frozen sections. Control mouse skin was stained for activated integrin ß1 and nidogen, a basal lamina marker (A), or for total integrin ß1 and nidogen (C). In the IIA KO epidermis both activated integrin ß1 (B) and total integrin ß1 (D) display suprabasal localization. Yellow arrowheads denote single basal layer of the epidermis that expresses integrin ß1 in the control epidermis, and the expanded suprabasal expression observed in the IIA KO epidermis. Staining for activated integrin ß1 was performed using antibody clone 9EG7 (upper panels) and total integrin ß1 was performed using antibody clone MB1.2, as previously described (Honda et al, 2007). Scale bar, 50 μm.

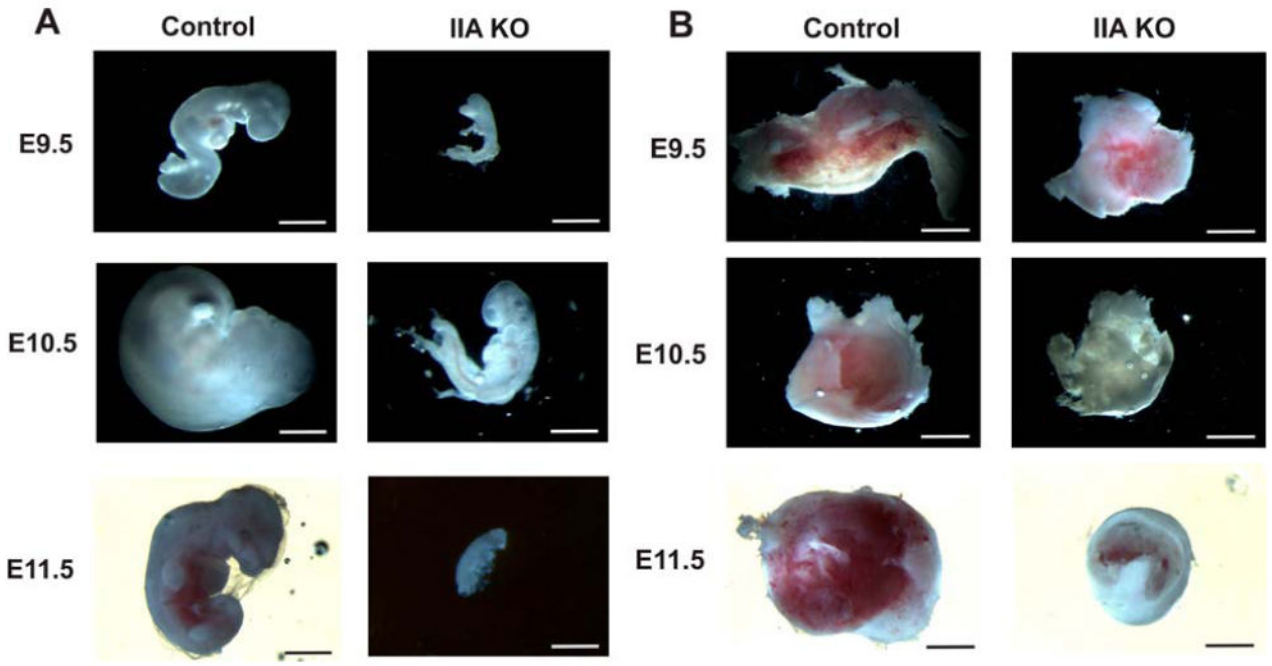

Figure 5. Embryonic lethality of the IIA KO embryos is underway by E9.5 and is associated with significant placental growth retardation

(A) Whole mount views of embryos at E9.5, E10.5 and E11.5. By E9.5 many IIA KO embryos show growth retardation and aberrant development. (B) Whole mount views of the corresponding placentas reveal reduced size and less vascularization. Scale bars, 1 cm.

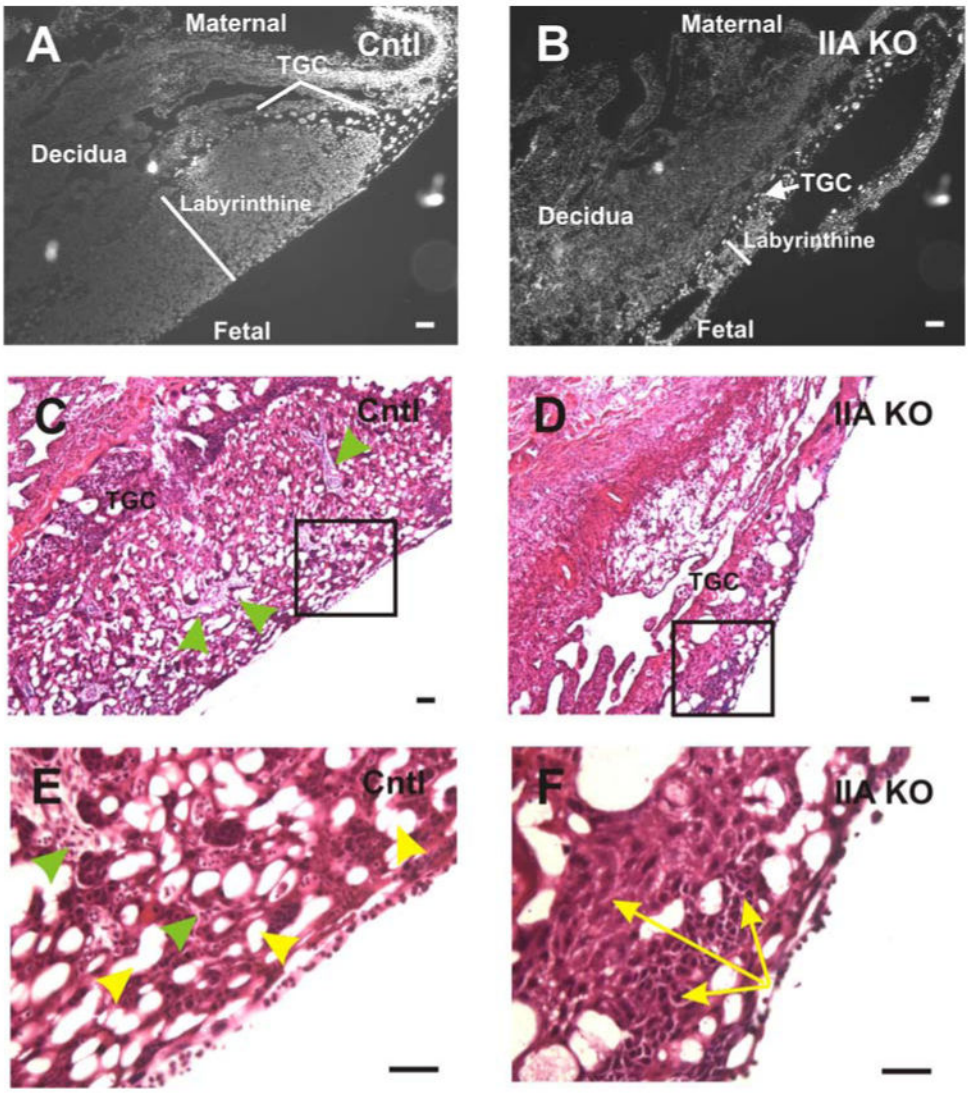

Figure 6. Placental defects are observed in the E12.5 IIA KO embryos

DAPI stained nuclei (gray scale) of control (A) and IIA KO (B) placentas. At E12.5, the IIA KO placenta exhibits a labyrinth whose area is dramatically reduced (white line) compared to the control placenta. The region of trophoblast giant cells (TGC) that normally surrounds the labyrinthine layer is thin and in some cases missing in the IIA KO placenta. H & E staining of control (C) and IIA KO (D) placentas reveals that the IIA KO placenta exhibits a lack of vascular infiltration originating from the maternal or fetal side, and a less porous network of sinusoidal spaces. The boxed regions in panels C and D are magnified in (E) and (F), respectively. The green arrowheads in (C) and (E) point to the well developed and organized trophoblast layer surrounding the vascular sinuses (yellow arrowheads, panel E) present in the control placenta. This ordered trophoblast cell-vascular sinus architecture is absent in the IIA KO placenta (F). Also, in panel F, the yellow arrows highlight a representative region of compacted trophoblast cells present throughout the labyrinthine layer of the IIA KO placenta but not evident in the control. Scale bars, 25 μm.

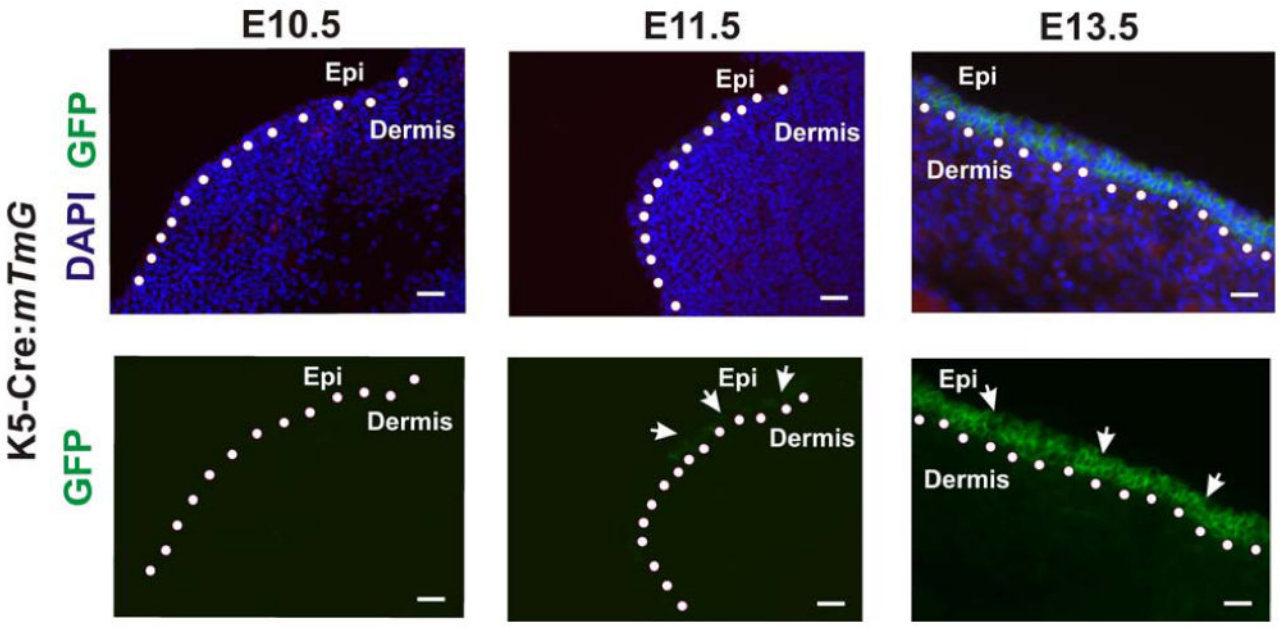

Figure 7. K5-Cre:mT/mG transgenic mouse demonstrates temporal- and epithelial-specific K5-Cre activation in the embryonic epidermis

K5-Cre:mT/mG embryos were harvested at E10.5, E11.5 and E13.5 days and the embryonic epidermis was isolated and cryosectioned. GFP expression was first detected as patches of expression in the developing epidermis at E11.5 and universally expressed in the epidermis at E13.5. White arrows indicate the epithelial-specific expression pattern of GFP, and dotted line indicates boundary between the epidermis and the dermis. Scale bars, 25 μm.

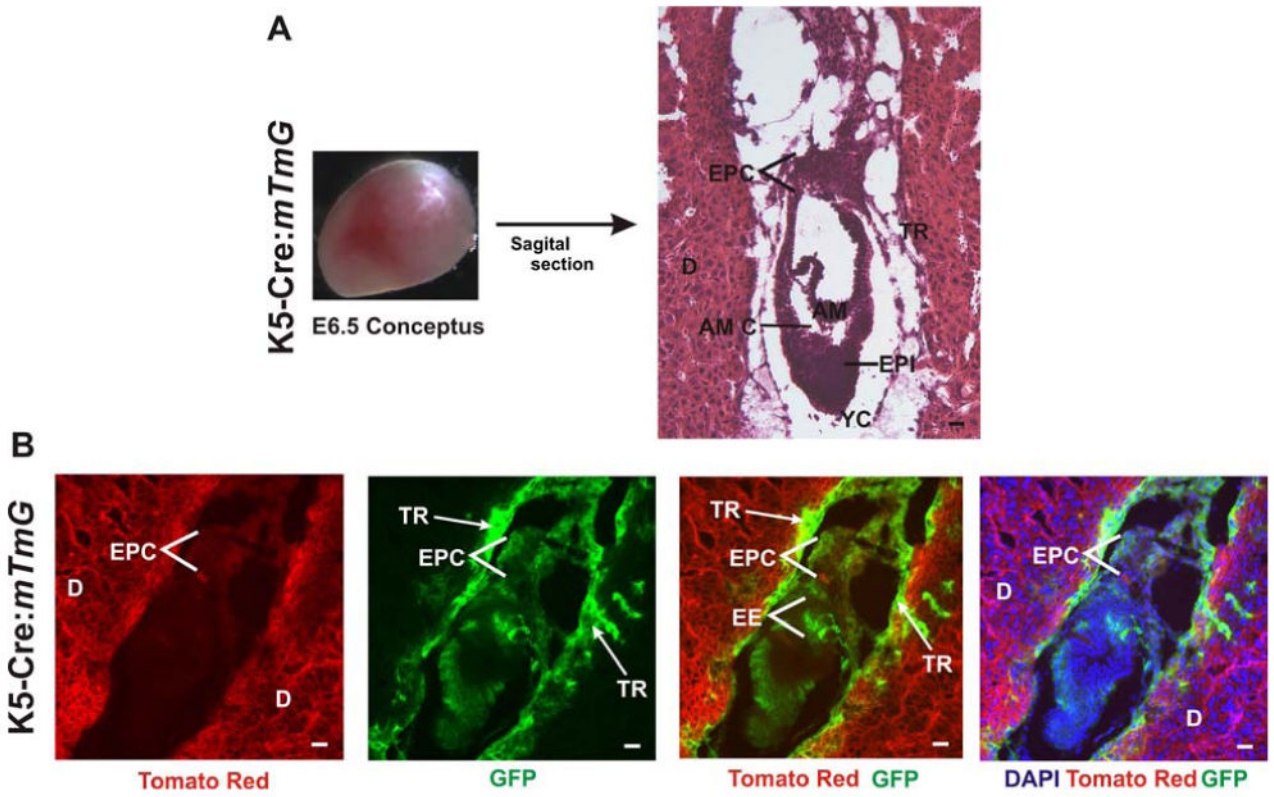

Figure 8. K5-Cre expression in E6.5 embryos in the ectoplacental cone, extraembryonic ectoderm and trophectoderm

(A) E6.5 conceptuses were harvested and sagittally sectioned. H&E stained sections show the decidua (D), ectoplacental cone (EPC), epiblast (EPI), Amniotic cavity (AM C), Amnion (Am), Yolk sac cavity (YC), and trophectoderm (TR). (B) GFP expression in K5-Cre:mT/mG E6.5 embryos. GFP is expressed in the ectoplacental cone, extraembryonic ectoderm (EE) and the trophectoderm. Scale bar, 25 μm.

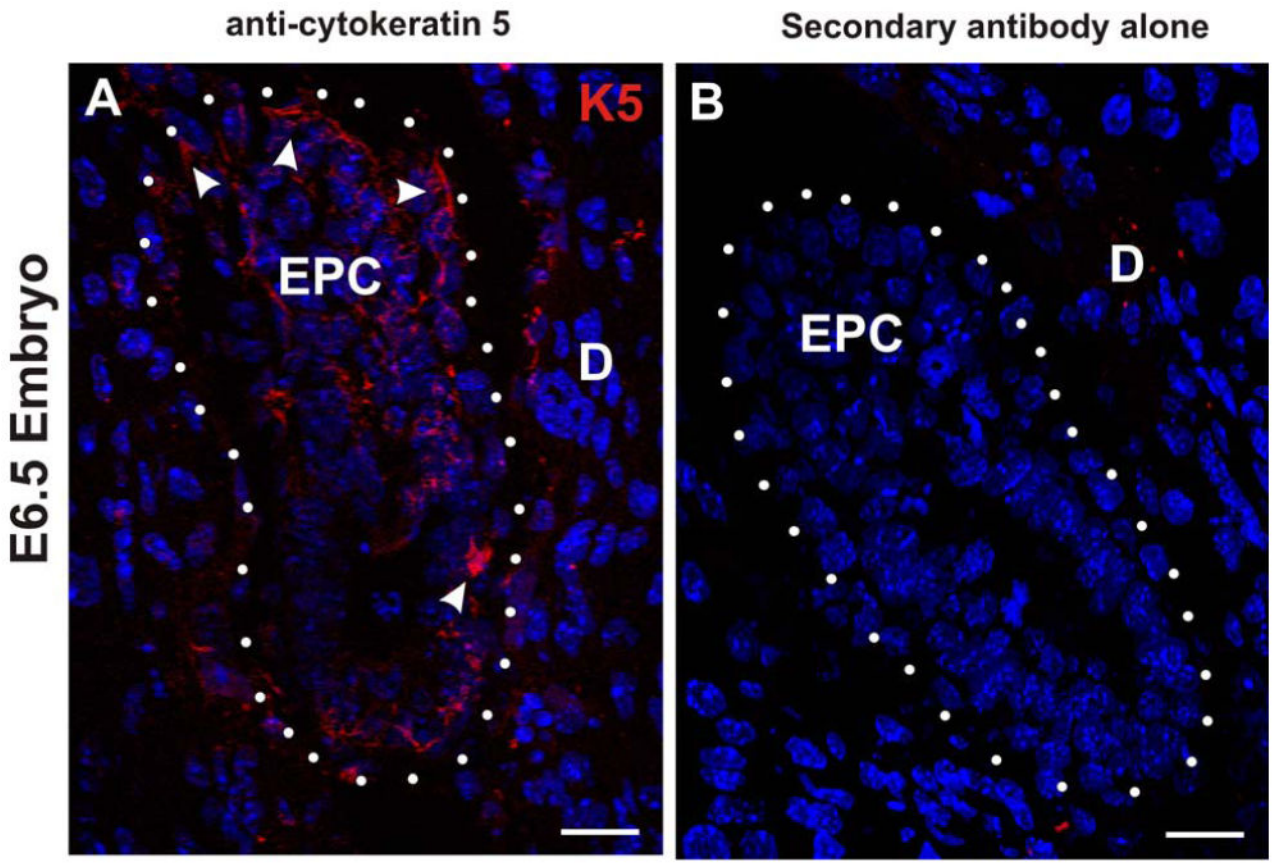

Figure 9. Endogenous cytokeratin 5 expression in the E6.5 embryo is observed in the ectoplacental cone and trophectoderm regions in control embryos

(A and B) Confocal immunofluorescence microscopy of frozen sections of E6.5 embryos. (A) Sagittal section of control E6.5 embryo was immunostained for cytokeratin 5 (K5; red) and stained with DAPI (blue). The white arrowheads identify K5 signal in the ectoplacental cone (EPC) and outer trophectoderm layer. The white dots enclose the embryo and denote the trophectoderm/decidua (D) border. (B) In the absence of primary antibody against cytokeratin 5 no immunostain signal is detected in the E6.5 embryo. Scale bars, 25 μm.

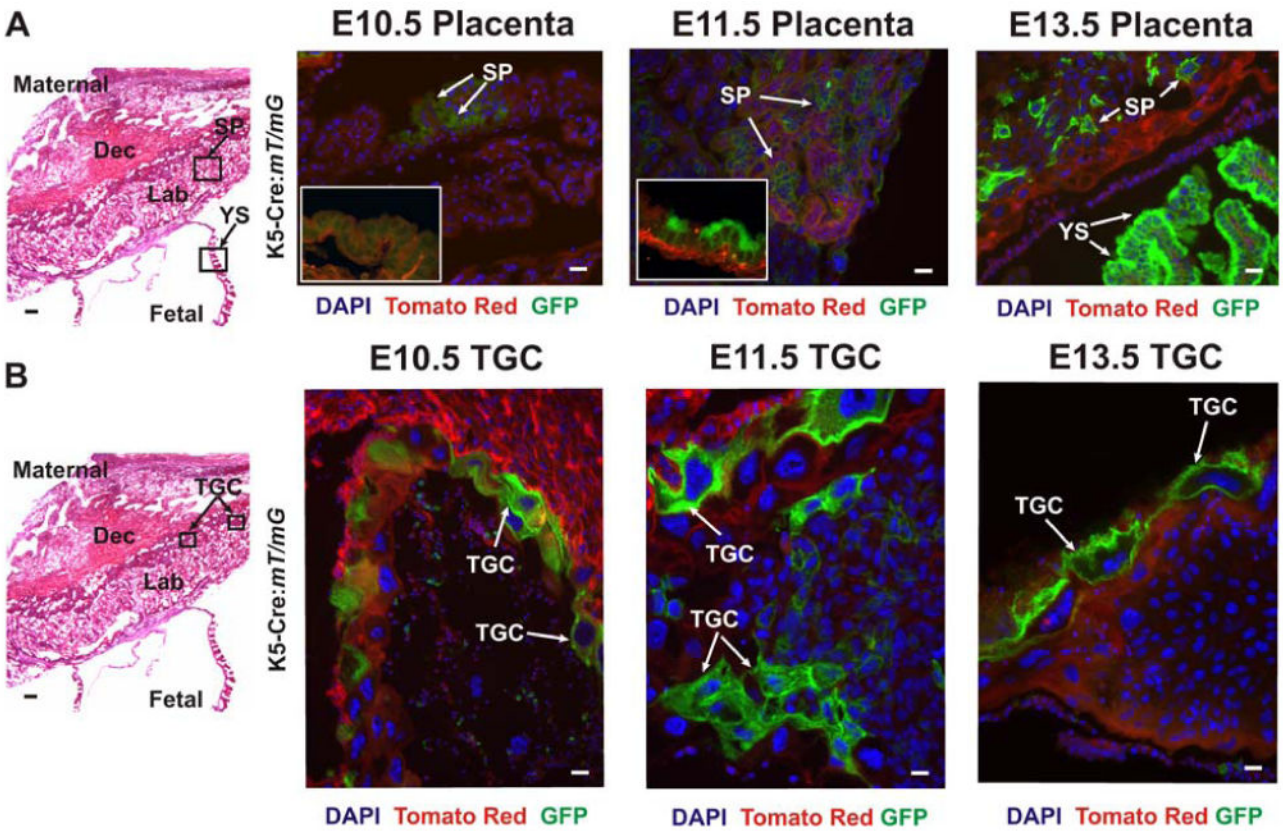

Figure 10. K5-Cre-mediated conversion of mT/mG transgene in the developing placenta demonstrates keratin 5 promoter activity in the trophectoderm lineages of TGC and labyrinthine trophoblasts, and in yolk sac

(A and B) The panels on the left are representative images of H&E stained placental sections, from E13.5. The boxed areas in these panels indicate zones that were examined at a higher magnification by fluorescence in other sections. Top Panels: E10.5, E11.5 and E13.5 placental sections were examined for GFP expression in the yolk sac (YS) and spongiotrophoblasts (SP) of the labyrinth. Insets for E10.5 and E11.5 show typical yolk sac stains at these time points. GFP (green), reflecting K5-Cre expression, is detected in the yolk sac in many fields of view at E13.5, in a scattered manner at E11.5, and was not observed in the yolk sac of E10.5 embryos. In spongiotrophoblasts, GFP was detected in many cells as early as E10.5. Lower panels: E10.5, E11.5 and E13.5 placental sections were also examined for GFP expression in the trophoblast giant cells (TGC). GFP expression is present by E10.5 and is also evident at the later stages (E11.5, E13.5) The white arrows indicate cells expressing GFP. Scale bars, 25 μm.

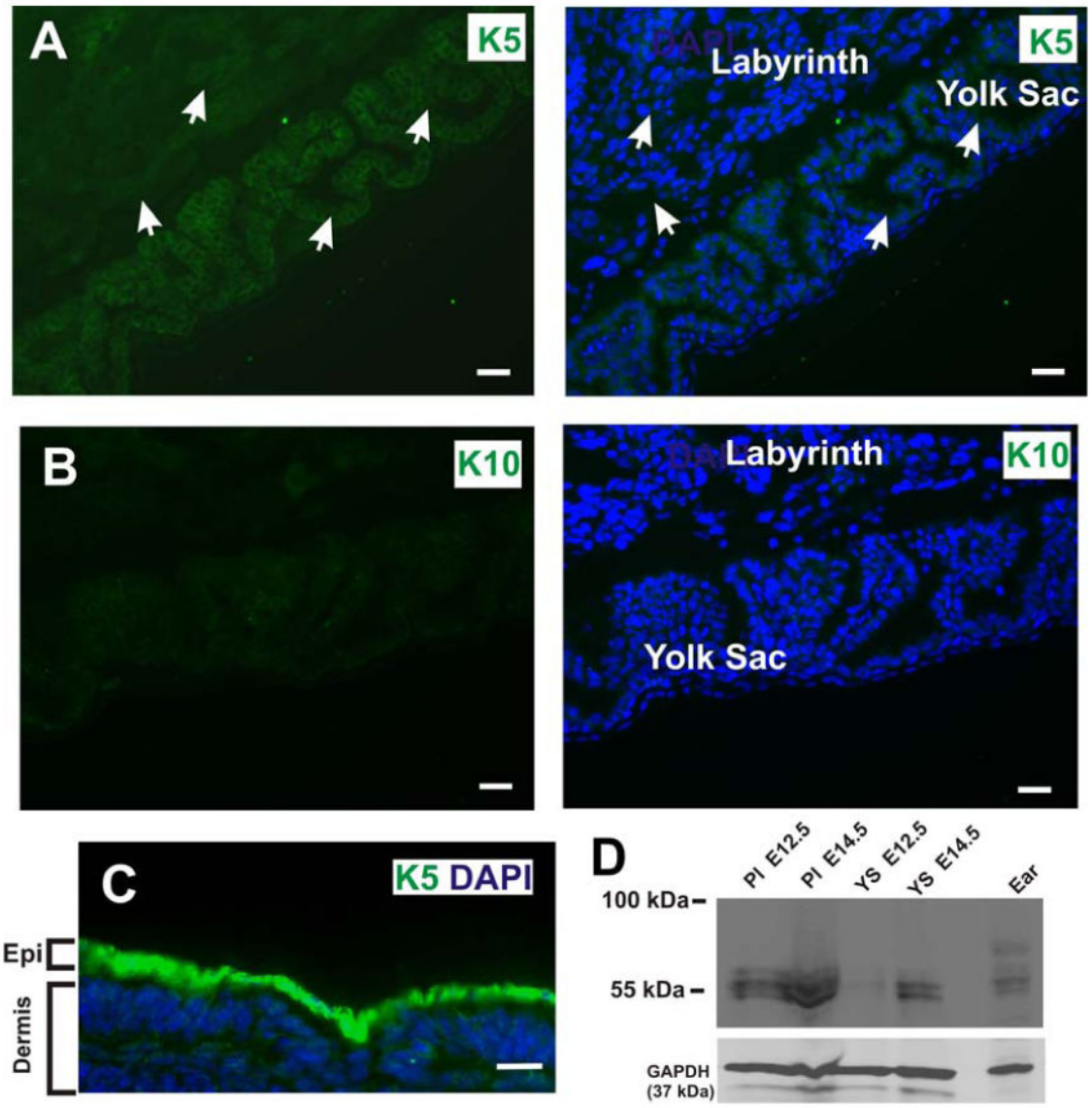

Figure 11. Endogenous cytokeratin 5 (K5) is detected in the labyrinthine layer and yolk sac of control E12.5 placentas

(A) The labyrinthine layer and yolk sac epithelia are derived from the trophectoderm and primitive endoderm, respectively. Wide field conventional immunofluorescence microscopy of frozen tissue sections of the E12.5 placenta revealed that the labyrinthine layer and yolk sac express endogenous K5, a basal cell marker. White arrows denote K5 expression in the labyrinthine layer and yolk sac. Blue is nuclear DAPI stain. (B) In contrast, no immunofluorescent signal is detected in the labyrinthine layer or yolk sac with an antibody against cytokeratin 10, a suprabasal marker. (C) Immunofluorescence staining of frozen cross section of E12.5 embryonic epidermis with a anti-cytokeratin 5 antibody (green). Scale bars, 25 μm. (D) Western blot of placenta (Pl) and yolk sac (YS) lysates at E12.5 and E14.5. Ear tissue lysate was used as a positive control for K5 expression. The lower portion of the same filter was probed for GAPDH as a loading control

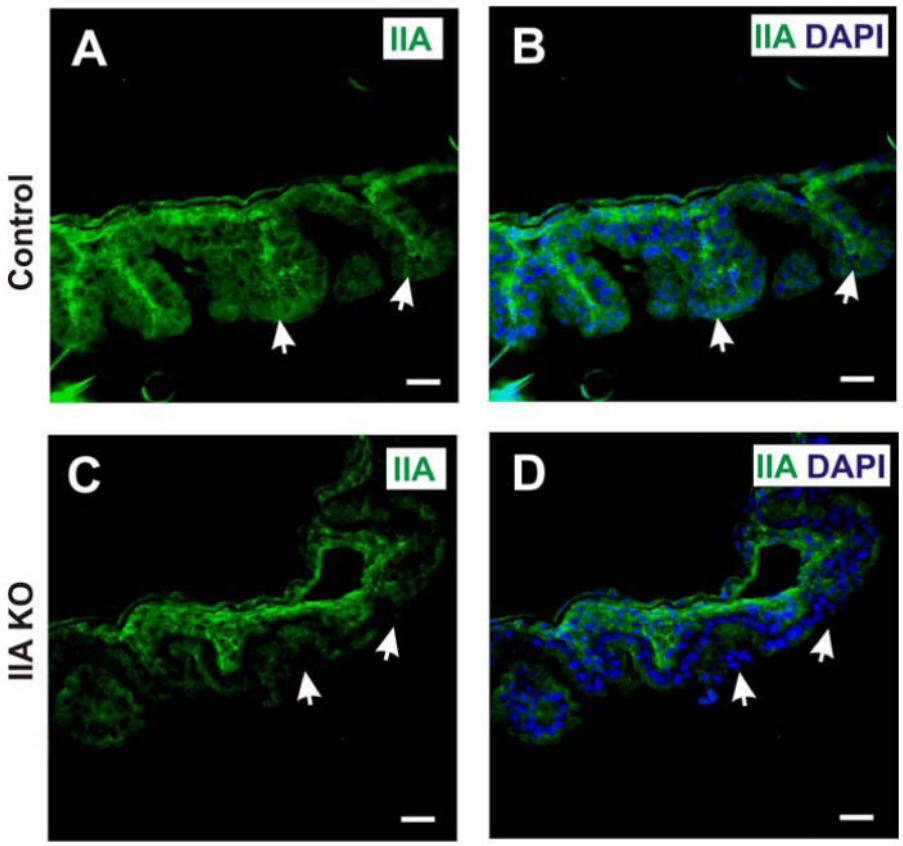

Figure 12. IIA KO mice exhibit diminished NMIIA expression along the cortical cell region of the yolk sac epithelium

Immunofluorescence staining of sections from the yolk sac of control (A,B) and IIA KO (C,D) embryos at E12.5 using antibody that detects NMIIA (green), with DAPI stain for nuclei (blue). White arrows indicate cortical staining of NMHC II-A in the epithelial cells of the control yolk sac (panels A and B), and diminished staining in IIA KO (panels C and D). Scale bars, 25 μm.

Table 1

Genotypic and viability analysis of offspring from K5-Cre/IIA$^{flox/+}$ and IIA$^{flox/flox}$ matings show a non-Mendelian distribution

Genotype	Viable Newborn at P1	Surviving Newborn	Expected Mendelian Genotypic Proportions	ObservedGenotypicProportions
K5-Cre/IIA$^{flox/flox}$	2	0	25%	∼1%
K5-Cre/IIA$^{flox/+}$	46	46	25%	32%
+/+/IIA$^{flox/flox}$	58	58	25%	40%
+/+/IIA$^{flox/+}$	38	38	25%	26%

Table 2

Frequency of embryo defects and reabsorption from K5-Cre/IIA$^{flox/+}$ and IIAflox/flox matings (17 litters total)

Embryonic Day	Reabsorbed & Defective Embryos	Intact Embryos	Total Embryos	% of Embryos Defective
E9.5	12	34	46	26%
E10.5	4	30	34	12%
E11.5	8	27	35	23%